DECAY SPECTROSCOPY OF HEAVY ISOTOPES AT SHIP USING THE COMPASS FOCAL PLANE DETECTION SET-UP*

A.K. Mistry[a,b], Z. Zhang[c], F.P. Hessberger[a,b], D. Ackermann[d]
B. Andel[e], S. Antalic[e], M. Block[a,b,f], P. Chhetri[a,g], F. Dechery[d]
C. Droese[h], Ch.E. Düllmann[a,b,f], F. Giacoppo[a,b], J. Hoffmann[a]
O. Kaleja[a,f], J. Khuyagbaatar[a,b], N. Kurz[a], M. Laatiaoui[a,b]
J. Maurer[a], P. Mošať[e], J. Piot[d], S. Raeder[a,b], M. Vostinar[d]
A. Yakushev[a]

[a]GSI Helmholtzzentrum für Schwerionenforschung, 64291 Darmstadt, Germany
[b]Helmholtz Institute Mainz, 55099 Mainz, Germany
[c]Institute of Modern Physics, Chinese Academy of Sciences
730000 Lanzhou, China
[d]GANIL, 14076 Caen, France
[e]Comenius University in Bratislava, 84248 Bratislava, Slovakia
[f]Johannes Gutenberg University, Mainz, Germany
[g]TU Darmstadt, Darmstadt, Germany
[h]Institut für Physik, Universität Greifswald, Greifswald, Germany

The new COMPASS detection system designed and developed at GSI, Darmstadt was employed in the focal plane of the SHIP velocity filter on-line during a period of commissioning. The isotope ^{254}No was initially measured for control purposes, following which the nuclei, ^{227,228,230}U, ^{229}Np, and ^{229,230}Pu were synthesized. The obtained data from α-decay spectroscopy is evaluated and compared with previous measurements.

1. Introduction

Decay spectroscopy of heavy and very heavy elements remains a crucial experimental method in identifying the location and ordering of single-particle energy levels which, in turn, provides a constraint for the models predicting the location of the closed spherical shell gaps for the heaviest nuclei.

See *e.g.* Ref. [1] for an in-depth review. This is done experimentally through well-established techniques such as decay spectroscopy, whereby the radiative emission of α particles, γ rays and internal conversion electrons (CE) are measured following implantation into the focal plane of gas- or vacuum-based ion-optic separators such as SHIP [2] and TASCA [3, 4]. Employing detection systems at the end of such large volume separators enables an almost background-free environment, as the primary beam used to produce such heavy nuclei (in fusion–evaporation reactions) is largely suppressed. As the experimental boundaries are pushed to increasingly challenging regions of the nuclear chart, where shorter lifetimes and lower production cross sections are a feature, it is necessary to upgrade existing experimental apparatus to more sophisticated set-ups with improved efficiency, granularity and timing resolution. To this end, the new COMPAct decay Spectroscopy set-up for SHIP (COMPASS) [5] was designed and constructed at GSI, Darmstadt, Germany in order to perform decay spectroscopy on heavy and superheavy nuclei. This report will give an overview of the commissioning of the detection set-up. For this purpose, ^{254}No was initially produced, with the daughter nucleus ^{250}Fm exhibiting a longer lifetime, to demonstrate the use of the improved granularity of the implantation detector. Following this, nuclei in a region of 'fast' decays around ^{230}Pu were studied in order to demonstrate the use of digital electronics. Additionally, both measurements have low production rates (maximum μb cross sections), and this combined with the long and short lifetimes demonstrates the necessary tools required for exploring the experimental sensitivity limits.

2. Experimental details

The study was performed in 2015/2016 with COMPASS coupled to the SHIP velocity filter [2]. A pulsed ^{48}Ca^{10+} beam was delivered from the UNILAC at a repetition rate of 5 Hz with 5 ms pulse length and impinged upon targets rotating synchronously with the beam frequency. The average beam current during the measurements was $I_{\text{beam}} \approx 85$ *p*nA on target. The two different targets used were carbon backed ^{208}PbS and $^{\text{nat}}$W material. The fusion–evaporation products were separated from the primary beam and other products by the filter, and delivered into the detection chamber mounted at the focal plane of SHIP. The detection system comprises a double-sided silicon-strip detector (DSSD) (60×60 strips, 1 mm strip pitch) manufactured by Canberra Semiconductors as the implantation detector surrounded by 4 single-sided silicon strip detectors (32 strips each) in a box formation to detect escaping α particles. A detailed description of the set-up can be found in Ref. [5]. The differential signals from preamplifiers developed at the Nuclear Physics Department of the University of Cologne, coupled to the detectors were sent to GSI in-house developed FEBEX pipelining ADC

modules for digital pulse processing. The first measurement for the purposes of calibration and optimisation of the set-up involved the reaction $^{48}\mathrm{Ca}(^{208}\mathrm{Pb},2n)^{254}\mathrm{No}$ at a beam energy of $E_{\mathrm{beam}} = 4.55\ \mathrm{MeV}/A$ for a period of 14 hours, the second, the irradiation of $^{\mathrm{nat}}\mathrm{W}$ at the same beam energy to produce isotopes of $^{227}\mathrm{U}$, $^{229}\mathrm{Np}$, and $^{229,230}\mathrm{Pu}$ in neutron and proton evaporation channels for a period of 65 hours.

3. On-line measurements

3.1. ^{254}No production

A total of 4010 $^{254}\mathrm{No}$ single event α particles were measured in the DSSD corresponding to a production cross section of $\sigma = (1.5 \pm 0.6)\ \mu\mathrm{b}$ compared with the previously measured value of $\sigma^{\mathrm{lit}} \approx 1.6\ \mu\mathrm{b}$ [6]. Figure 1 shows the α-decay spectrum recorded in the irradiation, the decay curves measured and the correlation to the daughter nucleus during the beam off
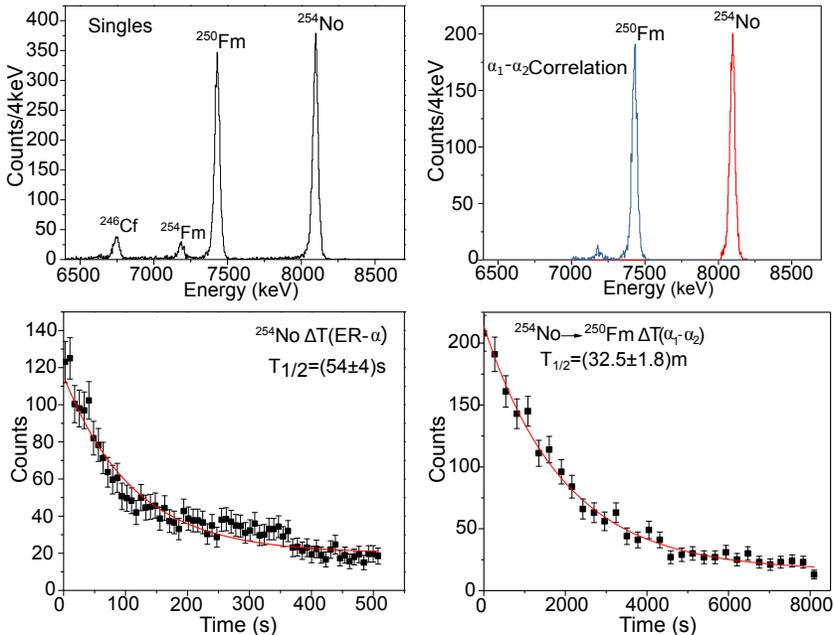
Fig. 1. (Colour on-line) Top left: $^{254}\mathrm{No}$ α-decay spectrum measured at SHIP in 2016 with the DSSD. Bottom left: $^{254}\mathrm{No}$ half-life measured between EVR implantation and α decay within $10 \times T_{1/2}$ of the literature value of $T_{1/2}^{\mathrm{lit}} = (51.2 \pm 0.4)$ s. Right top: α–α spectrum of $^{250}\mathrm{Fm}$ correlated to decays of $^{254}\mathrm{No}$ (red) within $6 \times T_{1/2}$ of $^{250}\mathrm{Fm}$. Right bottom: α-decay half-life of $^{250}\mathrm{Fm}$. Events were searched for in the same pixel in the beam off period.

period. The resolution (given as FWHM) was measured to be ≈ 35 keV. The evaporation residues (EVR) were identified using the implantation (DSSD) detector in combination with two Time-of-Flight (ToF) detectors mounted upstream of the detector chamber, with the EVR implantation energy in combination with the ToF used as a tag. The measured half-life following EVR implantation was $T_{1/2}(\text{EVR}–\alpha_1) = (54 \pm 4)$ s with literature values given as $T_{1/2}^{\text{lit}} = (51.2 \pm 0.4)$ s [7]. The subsequent α_1–α_2 correlation to ^{250}Fm daughter nucleus was measured at $T_{1/2}(\alpha_1–\alpha_2) = (32.5 \pm 1.8)$ m compared with the literature value of $T_{1/2}^{\text{lit}} = 30$ m [8]. The improved granularity of the new set-up with using the DSSD compared to the previous decay spectroscopy station at SHIP (which employed a 16-strip SSSD as the implantation detector) allows for longer decay times to be measured with a decreased random background rate.

3.2. Pu, U and Np isotopes

In order to demonstrate the performance of the device for nuclei exhibiting short lifetimes (100 ns $< T_{1/2} < 40$ μs), a number of isotopes were produced in the neutron deficient Pu region with the reaction ^{48}Ca$+^{\text{nat}}$W. With the use of digital electronics, the deadtime inherent for a conventional analogue electronics system is reduced to almost zero by recording each decay trace measured. Applying a trapezoidal filter (detailed in Ref. [9]) with adapted parameters in accordance to the length of the decay time allows the extraction of the energy deposited by particles in the detectors. Figure 2 gives an example of a decay trace observed for ^{222}Th$\rightarrow$ ^{218}Ra$\rightarrow$ ^{214}Rn stemming from the decay of ^{230}Pu. In grey/red the trapezoidal filter applied for extracting the energy is shown.
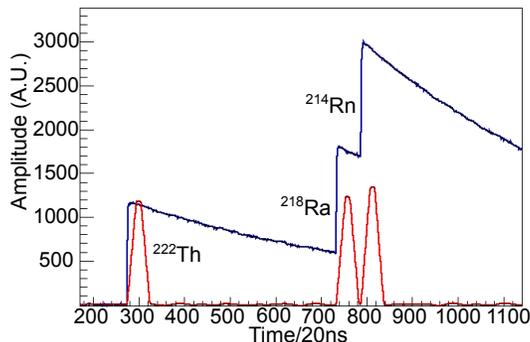
Fig. 2. (Colour on-line) An example trace (black/blue) of the triple pile-up signal ^{222}Th $(1.56$ ms$)\rightarrow^{218}$Ra$(9.17$ μs$)\rightarrow^{214}$Rn$(1.09$ μs$)$ with the energy resolved using the trapezoidal filter shown in grey/red, and the times given as the measured values in the shown trace.

For each chain, correlations were searched for within a number of seconds prior to, and after a pile-up event (*i.e.* two or more signals in the trigger window time of 40 μs) in the same pixel. Figure 3 shows the correlations between different chain members, with their assignment given as the starting isotopes of the chain, and two separate conditions applied. In the left panel for a correlation time of $\Delta T(\text{ER}–\alpha_1) < 510$ s and a second α-decay within $\Delta T(\alpha_1–\alpha_2) < 10$ s. The right panel shows the same as in the left panel, but with the correlation timings $\Delta T(\text{ER}–\alpha_1) > 510$ s and $\Delta T(\alpha_1–\alpha_2) < 10$ s and in the beam pause (off) period. Events with uncertain assignment are likely due to incomplete energy deposition (escaping α particles that were not detected by the upstream detectors), or random events during the beam on period.
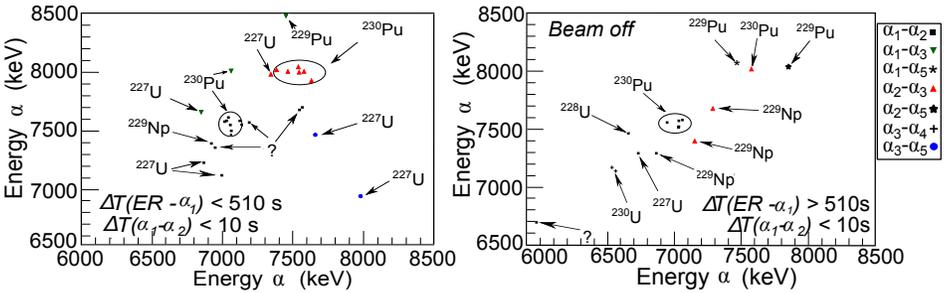
Fig. 3. Left: α–α matrix in a time range 510 s following an EVR implantation and a time difference $\Delta T(\alpha_1–\alpha_2)$ less than 10 s apart (beam pause and beam on). The measured decays depending upon the position in the chain they belong to (*e.g.* α_2–α_3) is indicated with different symbols given in the legend, and the chain they originate from is labelled. Right: The same as left but more than 510 s following implantation and in the beam pause period only showing longer lived decays.

From the initial implantation of ^{230}Pu, a total of 15 chains were assigned. Of these events, the majority were found to have a first α-decay energy of $E_\alpha = 7049(25)$ keV with one event at $E_\alpha = 7116(25)$ keV and another at $E_\alpha = 6931(25)$ keV. With the exception of the event at $E_\alpha = 7116(25)$ keV, this is consistent with the observations in Ref. [10] which attributed the decay of the lower energy α line ($E_\alpha^{\text{lit}} = 6999$ keV) to the α decay into the 2^+ state and the higher energy decay ($E_\alpha^{\text{lit}} = 7057$ keV) into the 0^+ ground-state in ^{226}U respectively. The decay of ^{226}U is known to have two α-decay branches which decay into the 2^+ ($E_\alpha^{\text{lit}} = 7387$ keV) excited state and into the 0^+ ($E_\alpha^{\text{lit}} = 7556$ keV) ground state of ^{222}Th. While the majority of the α-decay energies here are consistent again with Ref. [10], a single decay at $E_\alpha = 7450$ keV was measured which was not reported in Ref. [10], however

in Ref. [11], an α-decay line at $E_\alpha^{\text{lit}} = 7420$ keV was reported. Figure 4 shows the alpha-decay energies and time distributions of the events recorded for this chain.
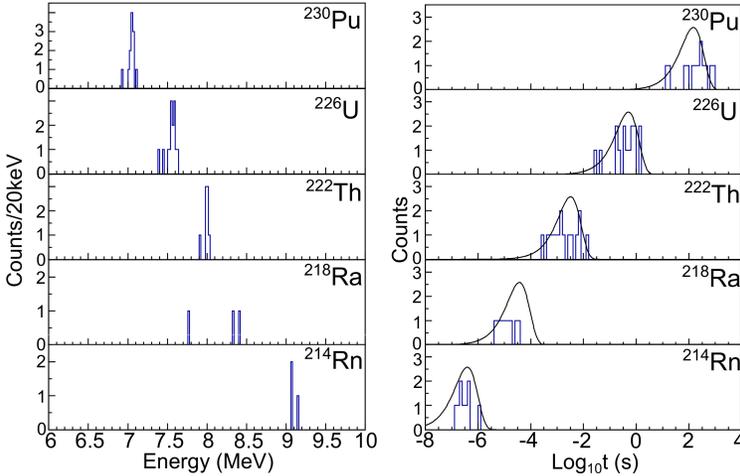
Fig. 4. Left: The α-decay energies of the decay chain originating from ^{230}Pu measured at SHIP. Right: α-decay half-life distributions of each member of the chain. The solid curves indicate the calculated time distributions for which the mean values are taken from literature.

The decay of ^{227}U was reported in Ref. [15] which aimed to measure the excited levels in ^{223}Th following the α decay of ^{227}U. In the study discussed in this report, 5 chains could be assigned to the decay of ^{227}U (with one escaping event). The α-decay energies (and half-lives) were found to be in agreement with those measured in Ref. [15] $E_\alpha^{\text{lit}} = 6864(3)$ keV, and $E_\alpha^{\text{lit}} = 6743(4)$ keV, here $E_\alpha = 6869(25)$ keV and $E_\alpha = 6742(25)$ keV. One additional α decay was observed at an energy of $E_\alpha = 7008(25)$ keV which is a result of α-CE summing (also observed in the aforementioned study). For ^{229}Np, three correlated chains were found, with one having an escaping ^{229}Np α decay. No electron-capture branch into ^{228}U was observed. The three chains originating from ^{229}Pu had α-decay energies and half-lives largely in agreement with the study reported in Refs. [25, 26] which measured the indirect production from ^{233}Cm. Finally, one chain could be tentatively assigned to the decay of ^{228}U ($E_\alpha = 6655(25)$ keV, $E_\alpha^{\text{lit}} = 6680(10)$ keV) albeit with escaping α particles in two members of the chain. Two events were assigned to ^{230}U, despite the long half-life ($T_{1/2}^{\text{lit}} = 20.23$ d) of the ^{230}U nucleus (measurement time 2.7 d). The data extracted is summarised in Fig. 5 which shows the chains measured in this study where more than

two events were observed. The literature values are given for comparison in the box with the measured values from this study given adjacent with uncertainties.

Chain 1 (^{230}Pu):

- ^{230}Pu — literature: 7.00(2), 7.06(1); measured: 7.12(3), 7.05(3), 6.93(3); t: 102(10)s; 200$^{+77}_{-43}$s
- ^{226}U — 7.57(1), 7.42(2), 7.39(1); 7.57(3), 7.45(3), 7.40(3); 0.27(1)s; 0.4(1)s
- ^{222}Th — 7.98(1), 7.60(1); 8.01(3), 7.92(3); 2.24(3)ms; 2.3$^{+0.8}_{-0.5}$ms
- ^{218}Ra — 8.39(1); 8.42(5), 8.33(5), 7.78(5); 25.2(3)μs; 9.9$^{+4.9}_{-2.5}$μs
- ^{214}Rn — 9.04(1); 9.16(5), 9.07(5); 0.27(2)μs; 0.26$^{+0.13}_{-0.06}$μs

Chain 2 (^{227}U):

- ^{227}U — 6.86(1), 6.90(1), 6.74(1); 7.01(3), 7.01(3), 6.87(3); 66(6)s; 57$^{+57}_{-19}$s
- ^{223}Th — 7.30(1), 7.29(1), 7.32(1); 7.32(3), 7.29(3), 7.38(3), 7.13(3); 0.6(2)s; 0.6$^{+0.5}_{-0.2}$s
- ^{219}Ra — 7.68(1), 7.99(1); 8.01(3), 7.92(3); 10(3)ms; 8.4$^{+8.4}_{-2.8}$ms
- ^{215}Rn — 8.67(1); 8.70(3); 2.3(10)μs; 2.9$^{+2.9}_{-1.0}$μs
- ^{211}Po — 7.45(1); 7.46(3), 7.09(3); 516(3)ms; 690$^{+690}_{-230}$ms

Chain 3 (^{229}Np):

- ^{229}Np — 6.98(2); 6.91(3); 240(12)s; 330$^{+460}_{-120}$s
- ^{225}Pa — 7.20(1), 7.25(1); 7.30(3), 7.16(3); 1.7(2)s; 2.6$^{+4.8}_{-1.0}$ms
- ^{221}Ac — 7.65(1), 7.44(2); 7.67(3), 7.40(3); 52(2)ms; 13$^{+23}_{-5}$ms
- ^{217}Fr — 8.32(1); 19(3)μs; 8.3μs
- ^{213}At — 9.08(1); 8.70(5); 0.125(6)μs; 0.18$^{+0.88}_{-0.08}$μs

Chain 4 (^{229}Pu):

- ^{229}Pu — 7.47(5); 7.48(3); 90$^{+7}_{-21}$s; 150$^{+240}_{-70}$s
- ^{225}U — 7.87(1), 8.47(1); 7.85(3); 69(15)ms; 130$^{+170}_{-70}$ms
- ^{221}Th — 8.47(1), 8.15(1); 8.51(3); 1.4(3)ms; 1.2$^{+5.6}_{-0.5}$ms
- ^{217}Ra — 8.99(1); 1.6(2)μs; 2.7$^{+13.0}_{-1.2}$μs
- ^{213}Rn — 8.09(1); 8.05(3); 19.5(1)ms; 18$^{+22}_{-8}$ms

Fig. 5. Summary of decay chains measured in this study where 3 or more events were recorded. The literature values are given in the boxes for the most intense α-decay paths, with the values measured for a given isotope in this study given in grey/red adjacent to the box. Energies are given in MeV. For ^{217}Fr and ^{217}Ra, no energy could be resolved. The literature references are as follows: ^{230}Pu [10], ^{226}U [11], ^{222}Th [12], ^{218}Ra [13], ^{214}Rn [14], ^{227}U [15], ^{223}Th [16], ^{219}Ra [17], ^{213}Rn [18], ^{211}Po [19], ^{229}Np [20], ^{229}Pu [25, 26], ^{225}Pa/^{225}U [21], ^{221}Ac/^{221}Th [22], ^{217}Fr/^{217}Ra [23], and ^{213}At/^{213}Rn [24].

4. Summary

The performance of the new COMPASS focal-plane detection system has been evaluated, initially through the measurement of ^{254}No testing its performance for longer correlation times with the increased granularity. Secondly, with the primary production being ^{230}Pu demonstrating the capabilities in the case of short decay sequences in the sub-μs region by using a digital system. The evaluation of the chains is in a good agreement with previously measured decays, where full chains could be evaluated, whereas before members of the chain have remained unrecorded due to deadtime of the electronics system.

REFERENCES

[1] M. Asai, F.P. Heßberger, A. Lopez-Martens, *Nucl. Phys. A* **944**, 308 (2015).

[2] G. Münzenberg *et al.*, *Nucl. Instrum. Methods* **161**, 65 (1979).

[3] A. Semchenkov *et al.*, *Nucl. Instrum. Methods Phys. Res. B* **266**, 4153 (2008).

[4] J. Khuyagbaatar *et al.*, *Phys. Rev. Lett. B* **115**, 242502 (2015).

[5] D. Ackermann *et al.*, published in *Nucl. Instrum. Methods Phys. Res. B* (2018) DOI:10.1016/j.nima.2018.01.096.

[6] F.P. Heßberger *et al.*, *Eur. Phys. J. A* **43**, 55 (2010).

[7] R.-D. Herzberg *et al.*, *Nature* **442**, 896 (2006).

[8] E. Browne, J.K. Tuli, *Nucl. Data Sheets* **112**, 1833 (2011).

[9] V.T. Jordanov, G.T. Knoll, *Nucl. Instrum. Methods Phys. Res. A* **345**, 337 (1994).

[10] P.T. Greenlees *et al.*, *Eur. Phys. J. A* **6**, 269 (1999).

[11] A.N. Andreev *et al.*, *Sov. J. Nucl. Phys.* **381**, 50:3 (1989).

[12] A.K. Jain, B. Singh., *Nucl. Data Sheets* **107**, 1027 (2006).

[13] S.-C. Wu, *Nucl. Data Sheets* **110**, 681 (2009).

[14] M.S. Basunia, *Nucl. Data Sheets* **121**, 561 (2014).

[15] Z. Kalaninova *et al.*, *Phys. Rev. C* **92**, 014321 (2015).

[16] E. Browne, *Nucl. Data Sheets* **93**, 763 (2001).

[17] B. Singh *et al.*, *Nucl. Data Sheets* **114**, 2023 (2013).

[18] B. Singh *et al.*, *Nucl. Data Sheets* **114**, 661 (2013).

[19] F.G. Kondev, S. Lalkovski, *Nucl. Data Sheets* **112**, 707 (2011).

[20] A.K. Jain, R. Raut, J.K. Tuli, *Nucl. Data Sheets* **110**, 1409 (2009).

[21] A.K. Jain *et al.*, *Nucl. Data Sheets* **108**, 883 (2007).

[22] Y.A. Akovali, *Nucl. Data Sheets* **100**, 141 (2003).

[23] M.S. Basunia, *Nucl. Data Sheets* **108**, 633 (2007).

[24] J. Chen, F.G. Kondev, *Nucl. Data Sheets* **126**, 373 (2015).

[25] P. Cagarda *et al.*, in: Proceedings of the 5th International Conference on Dynamical Aspects of Nuclear Fission, (Eds.) J. Kilman, M.G. Itkis, Š. Gmuca, World Scientific Publishing, 2002, p. 398.

[26] J. Khuyagbaatar *et al.*, *Eur. Phys. J. A* **46**, 59 (2010).